JOURNAL OF AGRICULTURAL AND FOOD CHEMISTRY

Dynamic Headspace Analysis of the Release of Volatile Organic Compounds from Ethanolic Systems by Direct APCI-MS

MAROUSSA TSACHAKI, ROBERT S. T. LINFORTH,* AND ANDREW J. TAYLOR

Samworth Flavor Laboratory, Division of Food Sciences, School of Biosciences, University of Nottingham, Sutton Bonington Campus, Loughborough LE12 5RD, United Kingdom

Static equilibrium headspace was diluted with a stream of nitrogen to study the stability of the volatile headspace concentration. The headspace dilution profile of 18 volatile compounds above aqueous and ethanolic solutions was measured in real time using atmospheric pressure chemical ionization-mass spectrometry. Under dynamic conditions the volatiles headspace concentration above water solutions decreased readily upon dilution. The presence of ethanol helped to maintain the volatile headspace concentration when the ethanol solution concentration was above 50 mL/L. This effect was such that under dynamic conditions the absolute volatile concentration above an ethanolic solution was higher than that above an aqueous solution, contrary to results observed in equilibrium studies. The ratio of the headspace concentration of volatiles above ethanolic 120 mL/L and water solutions was correlated to their air/water partition coefficient.

KEYWORDS: Dynamic; APCI; ethanol; interface; volatiles; wine; Marangoni

INTRODUCTION

Like many food products, the aroma character of alcoholic beverages is influenced by the volatile compounds that are present in the gas phase. Wine is an interesting example of an alcoholic beverage where the change in perceived aroma profile with time is well-documented. Indeed, the sensory description of wine aroma involves an appreciation of the initial aroma impact followed by a shifting pattern of flavor descriptors as the wine is taken into the mouth and then perceived via the transport of flavor compounds to the aroma and taste receptors.

Volatile release occurs through mass transfer of the volatile molecules from the liquid to the gas phase. In systems containing ethanol, aroma release is determined by the air−liquid partition (*1*), the presence of other solutes (*2*, *3*), and other physicochemical effects such as micelle formation (*4*) and surface tension effects (*5*). Ethanol increases solubility of volatiles (*3*) and consequently decreases their headspace concentration. Some studies only found an effect of ethanol on the partitioning of compounds when the ethanol concentration was higher than 170 mL/L (*6*, *7*). Other studies, however, demonstrated an effect on the headspace concentration of volatiles even below 170 mL/L ethanol solution concentration (*1*, *8*), which appears to be dependent on their hydrophobicity (*8*).

The studies reported above were carried out under static equilibrium conditions where the air/liquid partition is the key factor determining the headspace concentration. However, when people consume wine and other alcoholic beverages, the conditions are dynamic and therefore factors other than the air/liquid partition must be considered. The net effect of dilution and reequilibration is that the volatile profile of the headspace changes with time. Hence, there is a need to study the dynamic release profile of volatile compounds in order to understand release in real life situations.

Dynamic measurements of the gas-phase volatile content are possible with direct mass spectrometry techniques, such as atmospheric pressure chemical ionization-mass spectrometry (APCI-MS) and proton-transfer reaction-mass spectrometry (PTR-MS) (*9*, *10*). Dynamic headspace release studies allow real-time analysis of volatile headspace concentration above a solution as an inert gas dilutes the equilibrium headspace. They have been successfully used to understand the release of aroma compounds from aqueous solutions (*11*) or emulsions (*12*). The key factor affecting headspace stability was the air/water partition coefficient (K_{aw}); volatile molecules with lower K_{aw} values (10^{-4}) showed more stability during headspace dilution (*11*) than volatile molecules with higher K_{aw} values (10^{-2}).

The aims of the current study were to understand the effect of the presence of ethanol on volatile delivery for model solutions under dynamic conditions, as a first step in understanding the flavor release from wines and alcoholic beverages.

MATERIALS AND METHODS

Chemicals. Acetaldehyde, propanal, 2-butanol, diacetyl, 3-methyl-1-butanol, furfuryl alcohol, *c*-3-hexenol, ethyl-2-butenoate, phenylacetaldehyde, octanal, ethyl isovalerate, *p*-cymene, eucalyptol (1,8-cineole), and linalool were purchased from Sigma-Aldrich (Poole, U.K.); ethyl butyrate and (+)-limonene were obtained from Acros (Loughborough, U.K.); 1-octen-3-one was from Lancaster (Morecambe, England) and

* To whom correspondence should be addressed. Telephone: +44 1159 516144. Fax: +44 1159 516154. E-mail: robert.linforth@nottingham.ac.uk.

10.1021/jf051202n CCC: $30.25
Published on Web 09/16/2005

Table 1. Experimental and Physicochemical Properties of Volatile Compounds Used in This Study: Ion Measured (*m*/*z*); Optimum Cone Voltage (*V*) for APCI-MS Analysis Using Ethanol as the Charge-Transfer Agent; Range of Solution Concentration Used for the Analysis (μL/L); Average Relative Change in the Volatile Headspace Concentration of an Ethanolic Solution (120 mL/L) Relative to an Aqueous Solution (Mean Values and Standard Deviation of Three to Nine Replicates); and Air/Water Partition Coefficient (K_{aw})

volatile	*m*/*z*	V	μL/L	av rel change[a]	K_{aw}[b]
acetaldehyde	89	18	350–400	nd	2.727×10^{-3}
propanal	59	21	70–75	-7 ± 9	3.001×10^{-3}
2-butanol	57	24	8–10	-1 ± 9	3.704×10^{-4}
diacetyl	87	27	35–40	-4 ± 9[c]	5.437×10^{-4}
3-methylbutanol	71	21	50–55	-20 ± 4[c]	5.765×10^{-4}
furfuryl alcohol	81	30	350–400	-8 ± 6[c]	3.213×10^{-6}[d]
c-3-hexenol	101	18	350–400	-13 ± 3[c]	na
ethyl 2-butenoate	115	21	1.0–1.5	-20 ± 14	na
ethyl butyrate	117	21	1.5–2.0	-19 ± 4[c]	1.631×10^{-2}
phenylacetaldehyde	121	22	70–75	-31 ± 5	2.240×10^{-4}
1-octen-3-one	127	21	4.0–4.5	-33 ± 3[c]	na
octanal	129	21	4.0–4.5	-42 ± 3[c]	2.101×10^{-2}
ethyl isovalerate	131	21	1.5–2.0	-23 ± 3[c]	2.907×10^{-2}
p-cymene	134	24	0.5–1.0	12 ± 31	4.497×10^{-1}
limonene	137	24	1.5–2.0	9 ± 8[c]	1.051
terpinolene	135	30	4.0–4.5	-31 ± 9	5.724×10^{-1}
eucalyptol	155	12	4.0–4.5	-30 ± 3	4.497×10^{-3}
linalool	137	21	50–55	-33 ± 3[c]	8.790×10^{-4}

[a] Average relative change = ((volatile headspace concentration above ethanol solution)/(volatile headspace concentration above water solution) − 1) × 100. nd = not determined. [b] K_{aw} values calculated from Henry's law constant experimental values taken from EPI Suite software, U.S. Environmental Protection Agency. na = not available. [c] Data taken from ref *8*. [d] Because of the extreme value of Henry's Law constant found in the EPI Suite software database, the K_{aw} of furfuryl alcohol was measured as described in ref *11* with two different APCI-Mass Spectrometers and the average value of the two measurements, 3.650×10^{-5}, was used in Figure 3).

terpinolene from Fluka (Poole, U.K.). Ethanol (analytical reagent grade, 99.99%) was purchased from Fisher Scientific (Loughborough, U.K.). All volatile compounds were of 97% purity or greater apart from terpinolene and phenylacetaldehyde, which were of 90% purity.

Solutions. Individual solutions of the 18 volatile compounds were prepared in water. These solutions were then diluted with water or ethanol, to make the final water or ethanolic solutions, respectively. The volume of water and ethanol used was such that, for each individual volatile, its final solution concentration was the same in water and ethanolic solution (**Table 1**). The concentration used for each volatile was chosen with respect to its solubility in the solutions tested and its air/water partition coefficient, and it was within the infinite dilution range (*13*). Water solutions and ethanolic solutions of 120 mL/L were tested for all the volatiles. Ethyl butyrate, propanal, and 1-octen-3-one were tested in a range of ethanolic solution concentrations (0−230 mL/L).

APCI-MS. A Platform LCZ mass spectrometer was used, fitted with an MS Nose interface (Micromass, Manchester, U.K.) to sample the headspace above the solutions (*9*). The APCI source was operated with a modification as described previously (*8*) such that ethanol was added to the nitrogen makeup gas in a range of 2.0−11.3 μL/L N_2, depending on the ethanol concentration of the sample. This was done to ensure that the final concentration of ethanol in the source was the same whatever the ethanol concentration of the sample. The ethanol trimer $[M_3H]^+$ (ion 139) was monitored in every experiment to ensure a consistent concentration of ethanol in the source (the ethanol monomer and the dimer ions were beyond detection limits).

Selected ion monitoring (SIM) analysis was used for all experiments. Cone voltages and ions monitored for each volatile are shown in **Table 1**. Cone voltages were selected as the optimum cone voltages for the volatiles when ethanol reagent ions were used for the ionization. The ion used to measure each volatile was the most abundant species found in each case. This was typically the protonated molecular ion $[MH]^+$; but also included the molecular ion $[M]^+$; dimers $[M_2H]^+$; and the protonated molecular ion after dehydration $[M - H_2O + H]^+$.

Static and Dynamic Headspace Analysis. For static studies, 40 mL of volatile solution was placed in 123 mL flasks (Sigma-Aldrich) fitted with a one-port lid. After equilibration for at least 2 h at ambient temperature (22 °C), headspace was sampled through the port into the APCI-MS with a sample flow rate of 5 mL/min.

For dynamic studies, 100 mL of volatile solutions were placed in 123 mL flasks fitted with a two-port lid. After equilibration, N_2 was introduced through one port (70 mL/min) to dilute the headspace. As the gas flowed out of the second port, part of the gas flow was sampled into the APCI-MS (5 mL/min). The initial headspace concentrations observed at the start of dilution, as headspace started to be flushed out of the flask, were very similar to those observed in static headspace studies. The profiles were normalized to the signal intensity at the start of the time course (100%).

Statistical analysis was performed with Design Expert 6.0.6, Minneapolis, MN.

Stability of Ethanol Reagent Ions in the Source during Dynamic Headspace Analysis. Dynamic headspace analysis of the ethanol content of the headspace above ethanolic solutions of 0.1, 40, and 120 mL/L concentration were examined, with no addition of ethanol to the makeup gas flow. The headspace of 0.1 and 40 mL/L ethanol solutions were measured as described above for the dynamic headspace analysis of volatiles, the ions 47 and 139 (ethanol monomer and trimer, respectively) were monitored. For the 120 mL/L ethanol solution, a dilution device (dilution 1:400) was used to dilute the sample flow with nitrogen just before the sample entered the APCI-MS sampling line in order to keep the ethanol concentration within the detection limits of the APCI-MS (*m*/*z* 47 monitored).

RESULTS AND DISCUSSION

Ethanol Dynamic Headspace Dilution Profile. Ethanol affects the ionization of volatiles in charge-transfer reactions occurring in APCI-MS and PTR-MS techniques when the concentration exceeds 40 g/L (*9*, *10*). This effect can be eliminated by using ethanol as the mass-transfer reagent ion and maintaining a constant amount of ethanol in the source (*8*).

The dynamic headspace dilution device used in this experiment determined the capacity of volatiles to maintain their headspace concentration when a stream of nitrogen continuously diluted the headspace. It may have also affected the ethanol headspace concentration. If the amount of ethanol vapor entering the source in the sample gas changed substantially, it would be difficult to maintain a constant amount of ethanol in the source.

To determine the changes in the ethanol headspace profile, the ethanol headspace concentration above three different ethanolic solutions, 0.1, 40, and 120 mL/L was measured during gas-phase dilution. The ethanol headspace concentrations above 0.1 and 40 mL/L ethanolic solutions were very stable, remaining close to 100% and showing minimal variation (% CV = SD/mean × 100 = 6%) over the dilution phase (**Figure 1**). The headspace ethanol concentration above 120 mL/L was also stable but with higher variation (% CV = 20). This may have

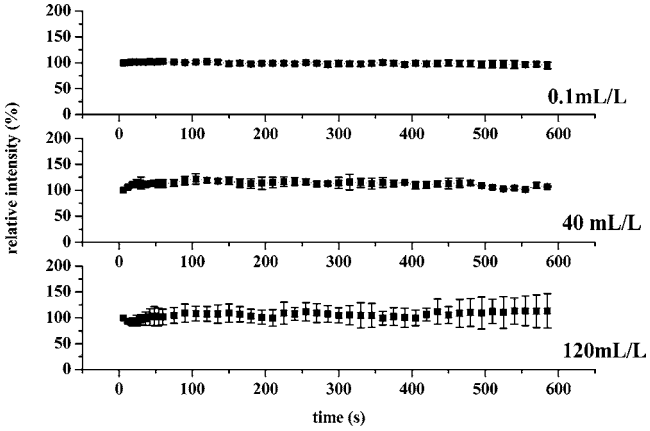

Figure 1. Average dynamic headspace dilution profiles of ethanol in the headspace above ethanolic solutions (0.1, 40, and 120 mL/L). Each point is the mean of three replicates; error bars show the standard deviation.

been caused by the variation in sampling flow rate due to the dilution device used.

Thus, the ethanol headspace concentrations above ethanolic solutions were effectively constant. Consequently, the ethanol concentration in the source will not vary substantially during headspace dilution analysis as a result of changes in the sample gas ethanol content. The amount of ethanol in the APCI source can be kept constant for all samples (whether they contain ethanol or not), by addition of ethanol to the makeup gas (*8*).

Marin and others (*11*) showed that changes in volatiles headspace concentration are related to the K_{aw} of volatiles. For compounds with low K_{aw} values (on the order of 10^{-5}) the volatile headspace concentration did not decrease readily upon dilution. Ethanol has a $K_{aw} = 2.04 \times 10^{-4}$, which is similar to that of diacetyl, $K_{aw} = 5.4 \times 10^{-4}$ (K_{aw} values calculated from experimental Henry's Law constant values taken from EPI Suite software, U.S. Environmental Protection Agency), and it would be expected to show similar behavior during headspace dilution. Diacetyl showed a decrease of around 30% during headspace dilution experiments (*11*). Ethanol, however, showed a very different profile from diacetyl with no apparent decrease during dilution. This suggests that there must be other factors apart from the K_{aw} influencing the overall mass-transfer coefficient of ethanol and consequently affecting its dynamic release. These factors are probably related to its ability to form a monolayer at the air/liquid interface (*14*).

Effect of Ethanol on Dynamic Headspace Dilution Profile of Volatiles. The behavior of volatile compounds during dynamic headspace dilution was associated with differences in the air/liquid partition coefficient (K_{al}) (*12*), when found in the range of infinite dilution (*13*). However, it normally needs at least an order of magnitude change in K_{al} for an effect to be observed. The K_{al} of volatiles in 120 mL/L ethanolic solutions was not much lower than that of volatiles in water solutions (**Table 1**). The majority of the volatiles showed a decrease in headspace concentration of less than 33% when dissolved in ethanolic solution compared to that observed when they were dissolved in water. Therefore we might expect the dynamic headspace concentration time profiles to be similar above ethanolic and aqueous solutions during gas-phase dilution.

The headspace concentration of ethyl butyrate above aqueous solutions showed a substantial decrease during headspace dilution (**Figure 2**). The final steady-state concentration after 600 s was 13% compared to the start of process. In contrast, when ethanol was present in the solution (120 mL/L), there was a similar depletion in ethyl butyrate headspace concentration for the first 18−24 s. After this time, the headspace concentration did not fall as quickly, and a final steady-state concentration equal to 75% of the initial concentration was obtained.

In static headspace studies the ethyl butyrate headspace concentration above ethanolic solution decreased by 19% compared to water solution (**Table 1**). Consequently, the absolute ethyl butyrate headspace concentration during dynamic headspace dilution analysis was actually higher above ethanolic than above water solutions. Ethanol in the solution appeared to help in maintaining ethyl butyrate delivery into the headspace.

Other volatiles also showed the same behavior as ethyl butyrate (**Figure 2**). In fact for the majority of the volatiles tested, the presence of ethanol in the solution helped to maintain the initial headspace concentration (**Table 2**) and hence increased their delivery into the headspace. Some of the volatiles tested showed very stable headspace concentration profiles during headspace dilution above water solutions (**Table 2**). Consequently, it was not possible to observe any additional impact of ethanol on their headspace stability.

The changes observed for the static equilibrium headspace concentration of volatiles above 120 mL/L ethanolic solutions compared to water solutions were related to their Log *P* value, an attribute linked to the hydrophobicity of the molecule (*8*). However, the results from the dynamic headspace dilution experiment did not show the same relationship. For example, ethyl butyrate, propanal, and eucalyptol showed very similar headspace dilution behavior although they have very different Log *P* values (**Figure 2**).

The three hydrocarbons tested, limonene, terpinolene, and *p*-cymene, behaved differently from the other compounds. Their headspace concentration profile above both water and ethanolic solutions showed a considerable decrease upon dilution (**Figure 2**, **Table 2**). The presence of ethanol did help to increase the headspace concentration by a factor of almost 10. However, the steady-state headspace concentration above aqueous solution was extremely low, less than 1% of the initial concentration (**Table 2**). Consequently, the presence of ethanol could not help to maintain the headspace concentration at levels as high as that of the other volatiles evaluated.

The ratio of volatile compounds headspace concentration at the end of the dynamic headspace analysis above the ethanol solution of 120 mL/L to water solution showed a sigmoid correlation with the K_{aw} value of the volatiles (**Figure 3**). Molecules with very low K_{aw} values, $\leq 10^{-4}$, such as furfuryl alcohol and linalool (**Table 1**), have stable headspace concentration above water solution during dynamic headspace concentration analysis (**Table 2**) due to their K_{aw} values. In this case, a very small benefit (diacetyl, 2-butanol, 3-methyl butanol) or no benefit at all (linalool, phenylacetaldehyde, *c*-3-hexenol) can be observed. The headspace concentration above the water solution of volatile molecules with K_{aw} values in the range of 10^{-3} to 10^{-2}, such as ethyl butyrate and eucalyptol, decreased readily upon dilution. In this case, the presence of ethanol in the solution helped to preserve the headspace concentration of volatiles in a steady state much closer to the equilibrium headspace. In this range of K_{aw} (10^{-3} to 10^{-2}) the correlation of K_{aw} to the ratio of volatile compounds headspace concentration at the end of the dynamic headspace analysis above the ethanol solution of 120 mL/L to water solution showed a linear profile (**Figure 3**). The dynamic headspace concentration of molecules with high K_{aw} ($\geq 10^{-2}$), such as hydrocarbons, above the water solution showed an extreme decrease upon dilution. This is probably because of the proportion of molecules that have to be transferred from solution to the gas phase as they try to reach equilibrium. Even above the ethanolic solution of

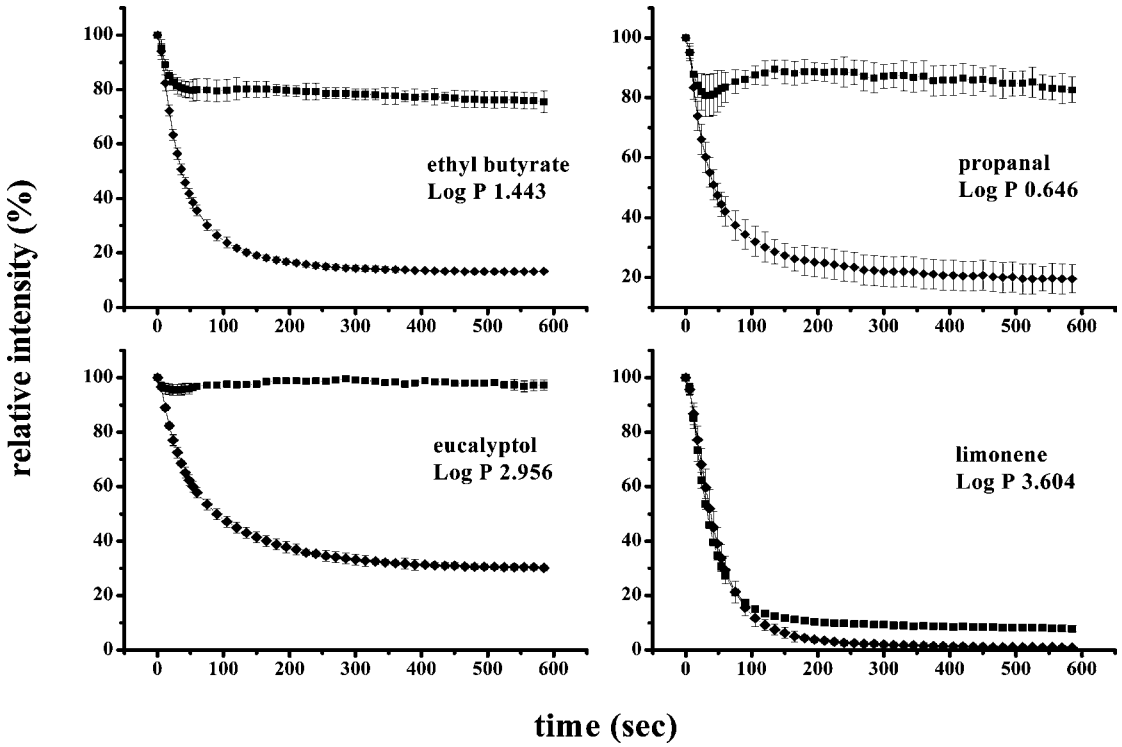

Figure 2. Dynamic headspace dilution profile of four volatiles in aqueous (◆) and ethanol (■) solutions (relative values). Each point is the mean of three replicates, error bars show standard deviation.

Table 2. Average Relative Intensity (%) of the Signal at the End of the Dynamic Headspace Dilution Analysis Relative to the Initial Intensity Prior to Dilution (100%) above Water and Ethanol (120 mL/L) Solutions[a]

volatile	water	ethanol
acetaldehyde	27.9 (5)	74.4 (17)
propanal	19.5 (24)	82.6 (5)
2-butanol	69.6 (5)	81.5 (5)
diacetyl	71.7 (5)	90.6 (7)
3-methylbutanol	75.9 (2)	89.5 (2)
furfuryl alcohol	95.6 (2)	92.6 (2)
c-3-hexenol	92.7 (1)	97.5 (1)
ethyl 2-butenoate	30.1 (3)	91 (5)
ethyl butyrate	13.3 (2)	75.5 (5)
phenylacetaldehyde	98.5 (1)	97.8 (0)
1-octen-3-one	34.4 (3)	96.6 (1)
octanal	8.6 (9)	49.2 (15)
ethyl isovalerate	5.5 (13)	52.5 (1)
p-cymene	0.9 (33)	11.9 (3)
limonene	0.9 (56)	7.9 (10)
terpinolene	0.8 (38)	7.0 (11)
eucalyptol	30.1(3)	97.3 (2)
linalool	92.2 (1)	96.7 (0)

[a] Values in brackets are the percentage coefficient of variation.

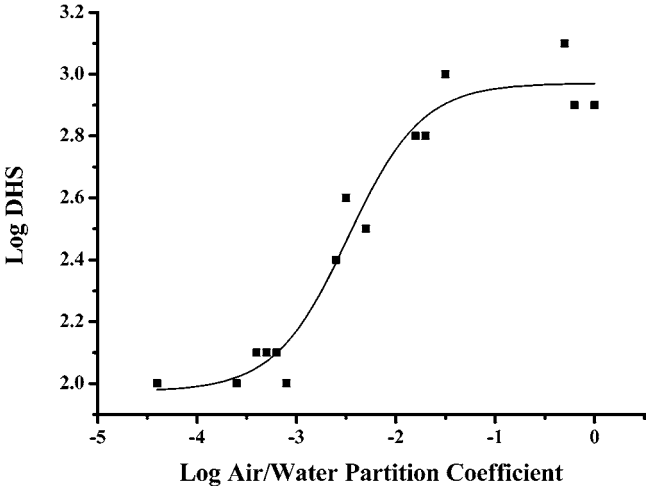

Figure 3. Logarithmic value (log DHS) of the ratio of volatile compound headspace concentration at the end of the dynamic headspace analysis above the ethanol solution of 120 mL/L to the water solution (DHS: (dynamic headspace concentration of volatile above ethanolic solution)/(dynamic headspace concentration of volatile above water solution) × 100) versus the logarithm of the air/water partition coefficient of the volatile compounds. Points represent experimental data; the line represents the sigmoid fit.

120 mL/L, the headspace concentration of volatiles with high K_{aw} showed a significant decrease upon dilution. As they are found at the very extreme limits of the high K_{aw} compounds ($>10^{-1}$) (**Table 1**), their behavior suggests that even with the benefit of better mass transfer due to the presence of ethanol, the molecules were leaving the surface of the solution much faster than they could be replaced by diffusion and convection. So, their headspace concentration was substantially depleted with or without ethanol.

Mechanisms of Volatile/Ethanol Interactions. The evaporation of a liquid occurs in two steps. First, the molecules of the bulk phase move to the surface (air/liquid interface), and second, these surface molecules escape into the gas phase (*15*). Thus, it should be expected that the dynamic headspace dilution profile is affected more by the surface volatile concentration than by the bulk solution volatile concentration.

Ethanol is surface active, and in ethanol/water solutions it adsorbs preferentially at the air/liquid interface, lowering the surface tension (*16*, *17*), at all alcohol concentrations (*18*, *19*). During the dilution of headspace with a stream of nitrogen, ethanol from the interface will start to evaporate. The evaporation from the interface of a fluid, such as water/ethanol, may lead to surface cooling resulting in some form of system instability. These can include Marangoni convection, which relies on the temperature dependence of surface tension (Ma-

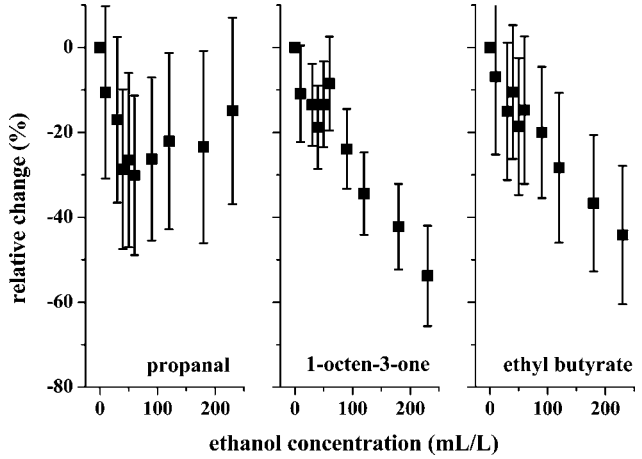

Figure 4. Relative change (%) in static equilibrium headspace concentration of volatile compounds above ethanolic solutions relative to ethanol solution concentration. Each point is the mean of three replicates, error bars show standard deviation.

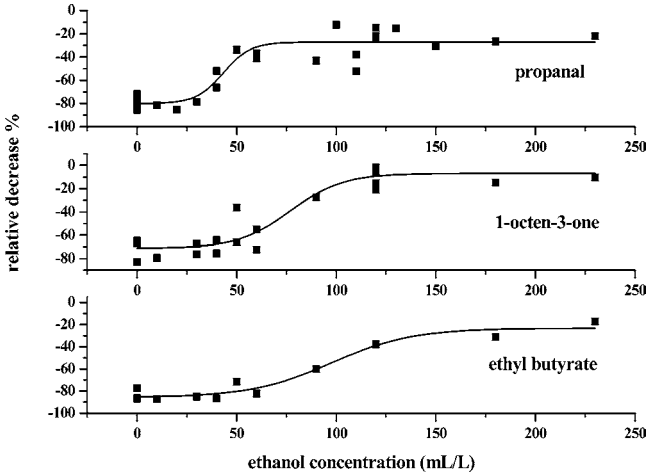

Figure 5. Relative decrease (%) of volatile headspace concentration at the end of the dynamic headspace analysis compared to headspace concentration at the start of the process versus the ethanol concentration of the solution. Points represent experimental data; the line represents the sigmoid fit.

rangoni effect), or Rayleigh−Bénard convection, which relies explicitly on the generation of buoyancy through the influence of temperature on fluid density (*20*). In a system such as water/ethanol, the evaporation of ethanol will also cause depletion of ethanol in some areas of the interface. This may further destabilize the system, resulting in chemical or compositional convection which may analogously follow either Marangoni or Rayleigh−Bénard mechanisms. However, the convective instability in an ethanol/water system is caused mostly due to an evaporatively driven thermal Marangoni convection (*20*, *21*).

According to the Marangoni effect mechanism, as ethanol evaporates, some depletion areas are produced in the interface with higher surface tension, due to the lower concentration of ethanol. This causes the molecules of the adjacent low surface tension regions to move toward the high surface tension region, carrying with them an appreciable volume of underlying liquid (*22*).

In our system, ethanol evaporated while the flow of nitrogen diluted the headspace. This caused surface tension gradients in the interface. Consistent with the Marangoni theory, ethanol molecules from the bulk moved to the interface to replenish the high surface tension areas. So, the interface was continuously replenished with ethanol molecules which could then escape to the vapor phase, at a constant rate. The replenishment was such that it could maintain the ethanol headspace concentration above the ethanolic solution steady during the whole duration of the dilution process. This is a possible explanation of why the ethanol dynamic headspace dilution profile did not show any decrease during dilution, contrary to results expected from its K_{aw} value. At the same time, volatile molecules from the bulk were dragged to the interface as the ethanol molecules moved to it. This led to a continuous flux of volatiles from the bulk to the interface, and hence it helped to preserve the headspace concentration of volatiles above ethanolic solution in a steady state much closer to the equilibrium headspace concentration, for the majority of volatile compounds.

Effect of Different Ethanol Concentrations on the Dynamic Headspace Profile of Volatiles. Although the variation in measurements was high, static headspace concentration of propanal above ethanolic solutions appeared to show a gradual decrease as ethanol solution concentration increased from 0 to 60 mL/L (**Figure 4**). Above a 60 mL/L ethanol solution, the static headspace concentration of propanal seems to be 30% lower than that observed above a water solution. Above 60 mL/L ethanol concentration the static headspace concentration showed no evidence of change with increasing ethanol concentration.

The effect of different ethanol concentrations on the relative decrease of volatile headspace concentration at the end of the dynamic headspace analysis compared to the headspace concentration at the start of the process was also evaluated. Dynamic headspace dilution concentration of propanal shows a short transition phase in the range of 30−60 mL/L ethanol solution concentrations (**Figure 5**). Below 30 mL/L ethanol concentration, the relative decrease of propanal headspace concentration at the end of the dynamic headspace analysis was similar to that observed above the water solution (**Figure 5**). Above 60 mL/L ethanol concentration (**Figure 5**), the relative decrease of propanal headspace concentration at the end of the dynamic headspace analysis showed no significant changes ($P > 0.05$).

1-Octen-3-one static headspace concentration appeared to show a small decrease at low ethanol concentration compared to aqueous solution, a plateau region from 10 to 60 mL/L, and then a gradual decrease with increasing ethanol concentration. Above an ethanol solution of 230 mL/L, the static headspace concentration of 1-octen-3-one was 54% lower of that observed for a pure aqueous solution (**Figure 4**). Dynamic headspace concentration of 1-octen-3-one above ethanolic solutions at different concentrations showed a smoother transition phase compared to that observed for propanal and in a different region, at 60−120 mL/L ethanol solution concentration (**Figure 5**). Below 60 mL/L the relative decrease (%) of 1-octen-3-one headspace concentration at the end of the dynamic headspace analysis was very similar to that observed for the water solution. Above 120 mL/L (**Figure 5**) the 1-octen-3-one headspace concentration at the end of the dynamic headspace analysis was very similar to that observed for the 120 mL/L ethanolic solution ($P > 0.05$).

Finally, ethyl butyrate equilibrium headspace concentration appeared to show a quite consistent decrease with the increase of ethanol solution concentration (**Figure 4**). Dynamic headspace concentration results of ethyl butyrate above different ethanolic solutions showed a smooth transition from 50 to 120 mL/L ethanol solution concentration (**Figure 5**). Below 50 mL/L ethanol concentration the relative decrease (%) of ethyl butyrate headspace concentration at the end of the dynamic headspace analysis was very similar to that observed above the water solution. Above that region the relative decrease of ethyl butyrate

headspace concentration at the end of the dynamic headspace analysis was very similar to that observed above the ethanol 120 mL/L solution ($P > 0.05$).

Results from static and dynamic headspace concentrations of the three volatiles described above gave evidence of a different behavior in relatively low ethanol concentrations, both at static and dynamic conditions. Many works have noted abnormal behavior of aqueous ethanol solutions at low ethanol concentrations (*21*, *23*). These differences may be due to changes in the bulk solution or the interfacial arrangement of molecules. Static headspace concentration of different volatiles at various ethanol solution concentrations have also been observed (*6*, *7*), but no results were given for ethanol concentrations below 50 mL/L, so no direct comparisons could be made. However, a two-step process was suggested (*7*), due to the presence of clathrate-like structures in the bulk solution (*23*).

On the other hand, the dynamic headspace profile of volatiles is also strongly related to the interfacial behavior of the solution, and one can expect that changes not only in the bulk solution but also in the interface are able to affect the dynamic release of the volatiles. Ethanol and water molecules have different orientations at the interface depending on the ethanol strength of the solution (*18*), and the orientational distribution of the water molecules at the liquid/gas interface plays an important role in determining the reactivity of the interface. As the concentration of ethanol increases from 55 to 125 mL/L, water molecules in the gas side of the interface shift to a smaller angle relative to surface normal in order to allow more ethanol molecules to adsorb in the finite number of available surface sites, yet the interface maintains the highly structured nature of the water surface. Above 125 mL/L ethanol concentration this highly ordered structure of water is abandoned in favor of adsorption of more ethanol molecules in the interface.

Even though it is difficult to draw direct correlations of the above results with ours, it is obvious that, at low ethanol concentrations, ethanol and water molecules in bulk solution and at the interface behave differently compared to higher ethanol concentrations. This can influence the behavior of other volatile molecules during both static and dynamic headspace analysis, depending on the properties of each volatile molecule.

Ethanol showed a significant enhancing effect for most of the volatiles under dynamic dilution conditions. This might have an important effect in the way ethanol influences the aroma profile of wine and alcoholic beverages, and it might be relevant when producing low alcohol content beverages. On the other hand, the effect of other solutes found in wine and alcoholic beverages on the dynamic headspace profile of volatiles also needs attention in order to determine their influence on volatile delivery from ethanolic solutions.

ACKNOWLEDGMENT

Greek State Scholarship Foundation (IKY) to M.T. and support of Firmenich SA for R.S.T.L. are acknowledged.

LITERATURE CITED

(1) Fischer, C.; Fischer, U.; Jakob, L. *Proceedings for the 4th international symposium on cool climate viticulture and enology*, 1996, New York State Agricultural Experiment Station: Geneva, New York, pp 42−46.

(2) van Ruth, S. M.; Villeneuve, E. Influence of beta-lactoglobulin, pH and presence of other aroma compounds on the air/liquid partition coefficients of 20 aroma compounds varying in functional group and chain length. *Food Chem.* **2002**, *79*, 157−164.

(3) Da Porto, C.; Nicoli, M. C. A study of the physico-chemical behavior of diacetyl in hydroalcoholic solution with and without added catechin and wood extract. *Lebensm.-Wiss. -Technol.* **2002**, *35*, 466−471.

(4) Conner, J. M.; Paterson, A.; Piggott, J. R. Agglomeration of ethyl-esters in model spirit solutions and malt whiskeys. *J. Sci. Food Agric.* **1994**, *66*, 45−53.

(5) Israelachvili, J. *Intermolecular and surface forces*; Academic Press: London, 1991.

(6) Escalona, H.; Piggott, J. R.; Conner, J. M.; Paterson, A. Effect of ethanol strength on the volatility of higher alcohols and aldehydes. *Ital. J. Food Sci.* **1999**, *11*, 241−248.

(7) Conner, J. M.; Birkmyre, L.; Paterson, A.; Piggott, J. R. Headspace concentrations of ethyl esters at different alcoholic strengths. *J. Sci. Food Agric.* **1998**, *77*, 121−126.

(8) Aznar, M.; Tsachaki, M.; Linforth, R. S. T.; Ferreira, V.; Taylor, A. J. Headspace analysis of volatile organic compounds from ethanolic systems by direct APCI-MS. *Int. J. Mass Spectrom.* **2004**, *239*, 17−25.

(9) Linforth, R. S. T.; Taylor, A. J. Apparatus and methods for the analysis of trace constituents of gases. 1999, U.S. Patent 5,869,344.

(10) Lindinger, W.; Hansel, A.; Jordan, A. On-line monitoring of volatile organic compounds at pptv levels by means of proton-transfer-reaction mass spectrometry (PTR-MS)—Medical applications, food control and environmental research. *Int. J. Mass Spectrom.* **1998**, *173*, 191−241.

(11) Marin, M.; Baek, I.; Taylor, A. J. Volatile release from aqueous solutions under dynamic headspace dilution conditions. *J. Agric. Food Chem.* **1999**, *47*, 4750−4755.

(12) Doyen, K.; Carey, M.; Linforth, R. S. T.; Marin, M.; Taylor, A. J. Volatile release from an emulsion: Headspace and in-mouth studies. *J. Agric. Food Chem.* **2001**, *49*, 804−810.

(13) Taylor, A. J. Physical chemistry of flavour. *Int. J. Food Sci. Technol.* **1998**, *33*, 53−62.

(14) Adamson, A. W.; Gast, A. P. *Physical chemistry of surfaces*, 6th ed.; Wiley-Interscience: New York, 1997.

(15) Myers, R. T. True molar surface energy and alignment of surface molecules. *J. Colloid Interface Sci.* **2004**, *274*, 229−236.

(16) Guggenheim, E. A.; Adam, N. K. *Proceedings of Royal Society − Series A*, **1933**, *139*, 218.

(17) Li, Z. X.; Lu, J. R.; Styrkas, D. A.; Thomas, R. K.; Rennie, A. R.; Penfold, J. The structure of the surface of ethanol−water mixtures. *Mol. Phys.* **1993**, *80*, 925−939.

(18) Stewart, E.; Shields, R. L.; Taylor, R. S. Molecular dynamics simulations of the liquid/vapor interface of aqueous ethanol solutions as a function of concentration. *J. Phys. Chem. B* **2003**, *107*, 2333−2343.

(19) Nishi, N.; Takahashi, S.; Matsumoto, M.; Tanaka, A.; Muraya, K.; Takamuku, T.; Yamaguchi, T. Hydrogen-bonded cluster formation and hydrophobic solute association in aqueous solutions of ethanol. *J. Phys. Chem.* **1995**, *99*, 462−468.

(20) Hosoi, A. E.; Bush, J. W. M. Evaporative instabilities in climbing films. *J. Fluid Mech.* **2001**, *442*, 217−239.

(21) Spedding, P. L.; Grimshaw, J.; Ohare, K. D. Abnormal evaporation rate of ethanol from low concentration aqueous- solutions. *Langmuir* **1993**, *9*, 1408−1413.

(22) Jaycock, M. J.; Parfitt, G. D. *Chemistry of interfaces*; Horwood: Chichester, U.K., 1981.

(23) Dangelo, M.; Onori, G.; Santucci, A. Self-association of monohydric alcohols in water—Compressibility and infrared-absorption measurements. *J. Chem. Phys.* **1994**, *100*, 3107−3113.

Received for review May 24, 2005. Revised manuscript received August 9, 2005. Accepted August 14, 2005.

JF051202N